## Full Length Article

# A facile one-pot synthesis and characterization of Ag$_2$Se nanoparticles at low temperature

CrossMark

*Delele Worku Ayele* *

*Department of Chemistry, College of Science, Bahir Dar University, P.O.Box 79, Bahir Dar, Ethiopia*

A B S T R A C T

A facile one-pot synthesis method has been developed successfully for the preparation of crystalline silver selenide (Ag$_2$Se) nanoparticles at low temperatures (5–7 °C) within few minutes. The method is based on the formation of phase separation and interface-reaction mechanism. During the synthesis, a microemulsion system (water/oleic acid/n-hexane) was used to make Ag$_2$Se nanoparticles. Selenium source (Sodium selenosulfate) used in this synthesis method was prepared by microwave heating due to the fact that the developed method of synthesis could eliminate toxic and expensive selenium sources. The prepared products (oleic acid coated Ag$_2$Se nanoparticles) were characterized by X-ray diffraction (XRD), energy-dispersive X-ray analysis (EDX), transmission electron microscopy (TEM), ultraviolet (UV)–visible analysis and photoluminescence (PL) analysis. The developed method became mild, fast, simple and environmentally benign, which would be helpful in scaling up production. Furthermore, the developed synthesis strategy could be used in making other nanoparticles for mass production through simple precipitation reactions.

## 1. Introduction

In past decades, silver selenide (Ag$_2$Se) has received great attention due to its special electronic and optical properties as well as potential applications [1–3]. Ag$_2$Se undergoes a polymorphic phase transition and has two stable solid phases. These are a low temperature orthorhombic phase (β-Ag$_2$Se) at 0 K, and a high temperature cubic phase (α-Ag$_2$Se) with a phase transition temperature from β to α-Ag$_2$Se taking place at about 135 °C or 409 K [2,4,5]. The low-temperature phase behaves as a semiconductor, while the high-temperature shows the properties of a metal. A low temperature phase (β-Ag$_2$Se) is a narrow band gap and n-type semiconductor with an energy gap of 0.07 eV at 0 K [5]. β-Ag$_2$Se is used as a photo sensitizer in photographic films or in thermo chromic materials and thermo electronic application due to its relatively high see back coefficient, low lattice thermal conductivity, and a high electrical conductivity [3,4,6–9]. The high-temperature phase (body-centered cubic), α-Ag$_2$Se, is a metallic compound with super ionic conductors that has been utilized as a solid electrolyte in photochargable secondary batteries and also used as an additive in highly conductive composite glasses for batteries, sensors, and displays [3,4,6–9].

* Tel.: +251936749196.
  *E-mail addresses:* delelewww@yahoo.com, delelew@bdu.edu.et.

Recently, research reports indicated that a slight tuning of the stoichiometry to $Ag_2Se$ could induce a remarkable magneto resistance, which is comparable to the giant magneto resistance perovskites [10–12]. Since nanoscale materials have some unique properties (that depend on the size and morphology of the particles) for a unique application [13,14], it would be a great challenge to fabricate $Ag_2Se$ nanostructures having uniform size and morphology. A number of methods for the synthesis of $Ag_2Se$ nanostructures have been explored [3,4,8,15,16]. All these routes to $Ag_2Se$ nanostructures, however, did not satisfy the criteria that the method be simple and fast, i.e., $Ag_2Se$ forms at low temperature in one step, and the prepared samples had nearly uniform morphology. Most of these $Ag_2Se$ synthesis routes have also used expensive and toxic selenium sources.

In this report, we employed a single step (the one pot) synthesis strategy to prepare uniform-sized $Ag_2Se$ nanoparticles at low temperature by reacting $Ag^+$ with $SeSO_3^{2-}$ under mild condition. In such synthesis approach, $Na_2SeSO_3$ was used as a selenium source since it could easily react with $Ag^+$ ions at room temperature without requiring the use of any other forms of energy [17]. $Na_2SeSO_3$ is much more active than Se powder, and is also less toxic, inexpensive and therefore safer to use than the $Na_2Se$ or $H_2Se$ [18]. $Na_2SeSO_3$ was prepared via microwave-enhanced method. A microwave-enhanced method, as opposed to conventional heating, has been proven to be an excellent technique for preparation of nanoparticles [18]. A few of the advantages of microwave-enhanced reactions include: simple to control the properties of the products, high yields of products, easy to control the temperature and pressure profile, the products have high purity levels, short reaction time, and environmental friendliness (e.g., improved safety, reproducibility, and selective heating, energy savings, etc.) [18]. A low-temperature microemulsion [19,20] environment was introduced to protect the prepared $Ag_2Se$ nanoparticles from aggregation and to direct them into a relatively uniform size. The low temperature reaction conditions also helped the formation of nearly monodisperse $Ag_2Se$ nanoparticles by slowing the growth speed and decreasing the surface atom activity.

The structure, morphology, elemental composition, and optical properties of the prepared $Ag_2Se$ nanoparticles were characterized by XRD, TEM, EDX, and UV–vis and Fluorescence spectrophotometer respectively. The developed synthesis method used very simple reagents such as oleic acid, $AgNO_3$ and $Na_2SeSO_3$ as precursors; was fast, easy/simple, mild, environmentally benign and of low temperature, which would be useful for large scale production and could be applied for the synthesis of other similar nanostructure materials.

## 2. Experimental section

### 2.1. Chemicals

Selenium powder (Se, 99.70%, <325 mesh), sodium sulfite ($Na_2SO_3$, >95%), and n-hexane (>99%) were bought from Acros; ethanol (>99%) and oleic acid (65–88%) were brought from Aldrich; Sliver nitrate ($AgNO_3$, >99%) and sodium hydroxide (NaOH, >95%) were bought from Shimakyus Pure Chemicals. The chemicals were used without further purification. The microwave system was employed for the synthesis of sodium selenosulfate ($Na_2SeSO_3$).

### 2.2. Synthesis of sodium selenosulfate ($Na_2SeSO_3$)

It was prepared in the laboratory using microwave-enhanced methods. The advantages of microwave heating over the conventional heating are explained above. Microwave (MW) synthesis was done by using a single-mode CEM Discover System operating at 300 W and 2.45 GHz. The reaction mixture was rapidly cooled with high-pressure air following termination of the reaction. $Na_2SeSO_3$ was prepared from sodium sulfite and selenium powder by microwave heating in aqueous solution for 30 min at 100 °C. For a typical preparation, selenium powder (0.4 g) and $Na_2SO_3$ (0.76 g) were dissolved in distilled water (50 mL); then, they were transferred to the microwave system. The following chemical reaction describes the formation of $Na_2SeSO_3$ under microwave system for 30 min reaction time at 100 °C.

$$Na_2SO_3 + Se \xrightarrow{MW(100°C \text{ and } 30\,min)} Na_2SeSO_3$$

Sodium selenosulfate ($Na_2SeSO_3$) was considered to be a greener selenium precursor than organic-based Se sources such as trioctylphosphine/Se or trioctylphosphine oxide/Se or others [18].

### 2.3. Synthesis of $Ag_2Se$ nanoparticles

The synthesis of $Ag_2Se$ nanoparticles was done in three steps. First step, NaOH (0.12 g) and oleic acid (2 mL) were dissolved in the mixture of deionized water (15 mL), $C_2H_5OH$ (15 mL), and n-hexane (1.5 mL) to form a transparent microemulsion. Second, AgNO3 (0.23 g) dissolved in deionized water (5 mL) was added to the solution (transparent microemulsion) under vigorous stirring, forming a white $Ag^+$ containing emulsion quickly. Third and the last step, after the emulsion had been maintained in the temperature range of 5–7 °C in the water bath, $Na_2SeSO_3$ solution (5 mL) was injected into it. The prepared solution changed its color from transparent to black in a few seconds, and stirring continued for up to 10 min.

After the reaction, n-hexane (20 mL) was added to destroy the microemulsion and extract the oleic acid-coated $Ag_2Se$ nanoparticles into the oil phase, which was centrifuged to give $Ag_2Se$ nanoparticles by adding $C_2H_5OH$. Then, the samples were washed more than three times by dissolving n-hexane coupled with precipitation from ethanol to remove oleic acid residues on the particle surface. Finally, the as prepared $Ag_2Se$ nanoparticles were dispersed in n-hexane for storage. The following chemical reaction describes the formation of $Ag_2Se$ nanoparticles with simple precipitation reactions.

$$Na_2SeSO_3 + 2AgNO_3 + H_2O \rightarrow Ag_2Se(s) + 2NaNO_3 + H_2SO_4$$
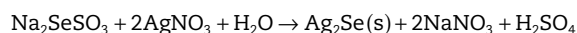
### 2.4. Characterization

Photoabsorption and photoluminescence measurements were performed by using a Jasco 560 UV/Vis Spectrophotometer and a Hitachi F-7000 Fluorescence spectrophotometer, respectively.

X-ray diffraction (XRD) measurements (Rigaku Model $D_{max}$-B, Japan) were recorded using a Cu Kα radiation source that was operated at 40 kV and 100 mA. The X-ray diffractogram was obtained at a scan rate of 0.05 deg $s^{-1}$ for 2θ values. The TEM images were obtained by using a Philips Tecnai 20 G2-field emission gun with a maximum acceleration voltage of 200 keV. The chemical composition of the $Ag_2Se$ nanoparticles was measured by energy-dispersive X-ray spectroscopy (EDX). FTIR spectra were recorded by using a Digilab FT3500 spectrometer (64 scans with a resolution of 4 $cm^{-1}$).

## 3.    Results and discussion

Fig. 1 shows the XRD patterns of $Ag_2Se$ nanoparticles obtained at the reaction times of 10 min and particle-growth temperatures of 7 °C. As seen in Fig. 1, the as-prepared $Ag_2Se$ nanoparticles sh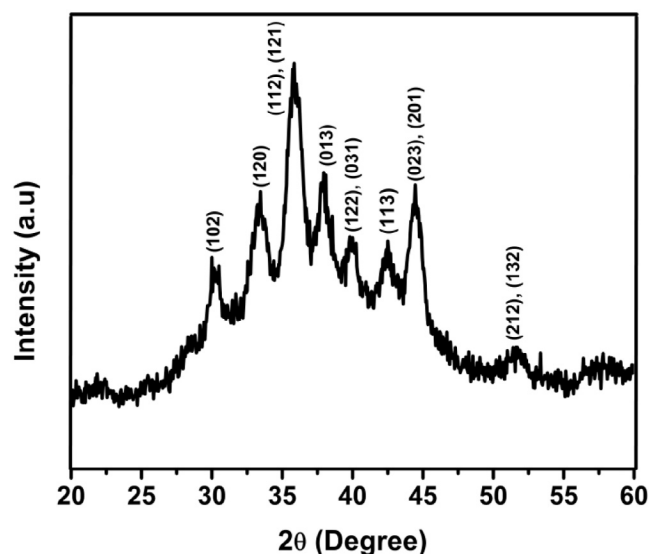ow characteristic peaks of orthorhombic phase of β-$Ag_2Se$. All the characteristic peaks, seen in Fig. 1, correspond to the orthorhombic phase of β-$Ag_2Se$, which is in good agreement with the literature data for β-$Ag_2Se$ (the standard JCPDS card File, 24–1041). As reported in literature [16,21–26], it seems also logical to produce the orthorhombic phase at low temperature since it is a low-temperature stable phase. A slight peak broadening, shown in the XRD patterns, may reflect the smaller particle size (around 8 nm) of the products.

Fig. 2a and b shows the TEM images of the as-prepared products at different magnifications. The products are nearly monodisperse without any aggregation with the particle size ranges from 6 to 10 nm. The average particle size is calculated to be 8 nm. The high-resolution transmission electron microscopy (HRTEM) images in the inset of Fig. 2b show the lattice spacing of ~0.24 nm, corresponding to the characteristic of the (013) crystal planes of β-$Ag_2Se$ nanoparticles [27,28].

Fig. 3 shows the Energy Dispersive X-ray (EDX) spectrum taken from the selected area of SEM images (seen in the inset figure in Fig. 3). The result of the EDX shows that the atomic ratio of the Ag and Se in this tubular product is 66.33:33.67, close to the stoichiometric composition of the $Ag_2Se$. Thus, the atomic composition of Ag and Se, in the as-prepared products, is merely similar to the stoichiometric composition of $Ag_2Se$.

Fig. 4 shows the FTIR spectra of the as-prepared $Ag_2Se$ nanoparticles and the pure oleic acid (OA). FTIR spectroscopy can offer insight about the interaction between the oleic acid and the $Ag_2Se$ nanoparticles. The broad peak between 3500 and 2500 $cm^{-1}$ was observed in the pure oleic acid spectra, which is clearly due to the O—H stretch of the carboxylic acid [29–33]. Such a broad and intense band at high wave number is a typical characteristic of O—H functional group of the carboxylic acid. However, the as-prepared $Ag_2Se$ nanoparticles have no such bands in this region indicating that the oxygen atoms in O—H groups were chemisorbed on the surface of $Ag_2Se$ nanoparticles. A pure oleic acid spectra show two sharp bands at 2925 and 2857 $cm^{-1}$, which were superimposed on the O—H stretch, and were attributed to the asymmetric $CH_2$ stretch and the symmetric $CH_2$ stretch of the free OA, respectively [29–31,34]. When oleic acids were chemisorbed on the surface of $Ag_2Se$ nanoparticles, the asymmetric $CH_2$ stretch and the symmetric



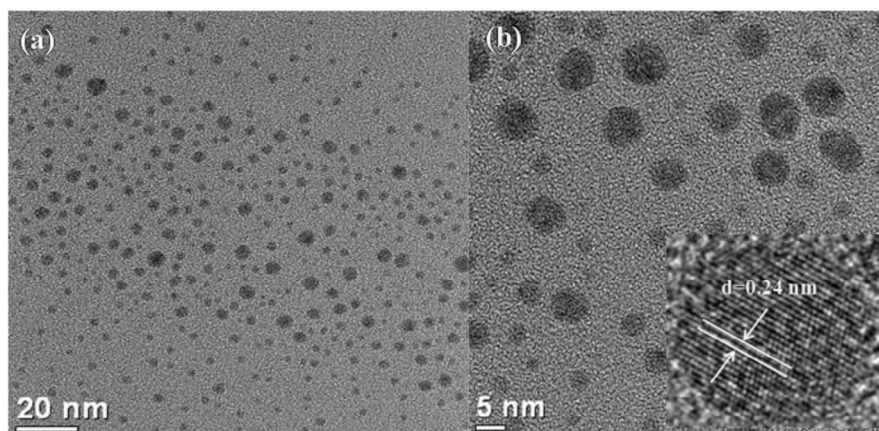**Fig. 1 – XRD patterns of $Ag_2Se$ nanoparticles.**



**Fig. 2 – TEM images (a & b at different magnification) of $Ag_2Se$ nanoparticles. The inset figure in (b) shows the HRTEM images with the lattice fringe spacing of ~0.24 nm.**
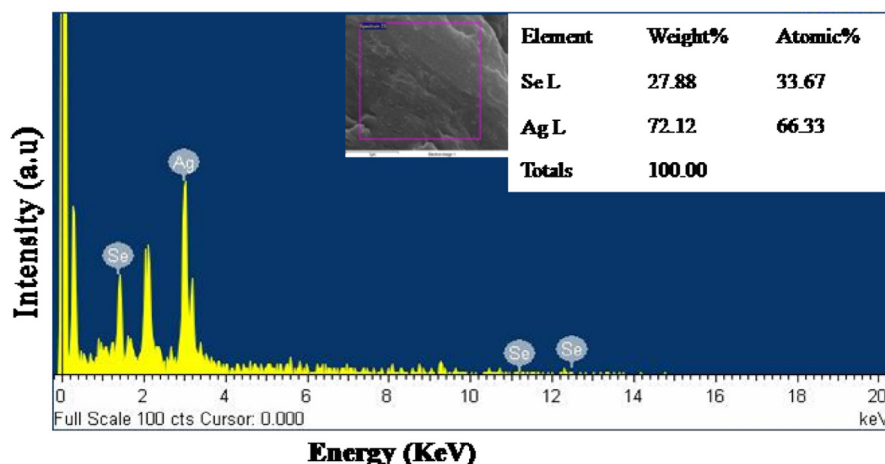
**Fig. 3 – Energy Dispersive X-ray (EDX) spectrum of Ag₂Se nanoparticles. The inset figure gives the selected area for EDX measurement and the chemical composition of Ag₂Se nanoparticles.**

CH$_2$ stretch shifted to 2919 and 2851 cm$^{-1}$, respectively, as shown in the FTIR spectra of Ag$_2$Se nanoparticles (Fig. 4).

In the pure oleic acid spectra, the intense peak at 1710 cm$^{-1}$ was due to the presence of the C═O stretch, and the band at 1285 cm$^{-1}$ that indicated the presence of the C—O stretch [29–31]. In addition, the O—H in-plane and out-of-plane bands of the pure oleic acid appeared at 1463 and 934 cm$^{-1}$, respectively [29–31]. These bands disappeared in Ag$_2$Se nanoparticles shown in Fig. 4, instead, two new bands at 1550 and 1440 cm$^{-1}$ appeared, which are characteristic of the asymmetric $v_{as}$(COO$^-$) and the symmetric $v_s$(COO$^-$) stretching [29–31], respectively. The results from FTIR spectra in Fig. 4 reveal that oleic acid was chemisorbed, as a carboxylate ion, onto the surface of the as-prepared Ag$_2$Se nanoparticles (oleic acid capped Ag$_2$Se nanoparticles or OA-capped Ag$_2$Se), and that the two oxygen atoms in the carboxylate were coordinated symmetrically to both the Ag and the Se atoms.
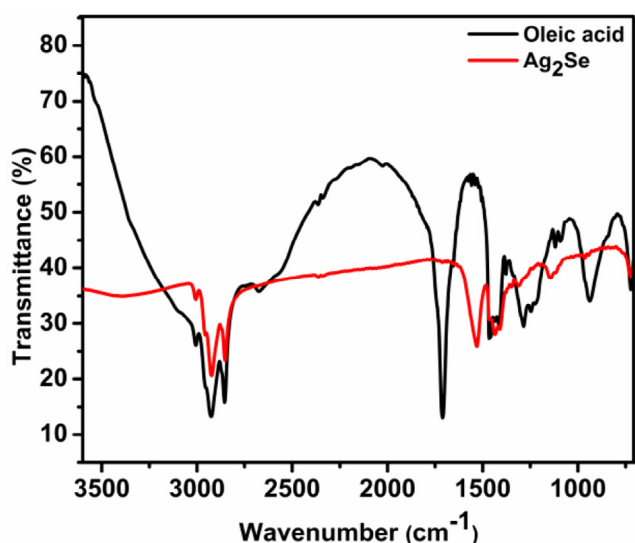
Based on the aforementioned experimental results, it seems possible to explain the role of oleic acid in such synthesis strategy of Ag$_2$Se nanoparticles. First, oleic acid and silver nitrate essentially lead to the formation of a silver oleate intermediated by replacing the nitrate group in the starting materials. Second, Se$^{-2}$ is generated by the reaction of SeSO$_3^{-2}$ with OH$^-$. Third, the intermediate silver oleate reacts with Se$^{-2}$ to form Ag$_2$Se nanoparticles surrounded by oleate groups. This method protects the nucleation of the tiny particles, as shown in the following schematic diagram below (Scheme 1).

In general, capping ligands could prevent the aggregation of small crystals and influence the morphology of the as-prepared nanoparticles. The dynamics of the surface ligands attached and detached could be varied by controlling the temperature and the nature of the ligand. Thus, the reaction temperature could be used to control the growth of nanocrystals.

To further confirm the formation of Ag$_2$Se nanoparticles and understand its optical properties, UV–visible absorption and photoluminescence (PL) measurement of the as-prepared Ag$_2$Se nanoparticles in n-hexane were performed. Fig. 5 shows the UV–visible absorption: (a) photoluminescence; (b) spectra of oleic acid capped Ag$_2$Se nanoparticles.

As seen from Fig. 5a, the absorption edge was determined at around $\Lambda = 635$ nm, which is close to the literature value ($\Lambda = 629$ nm) [21] reported for Ag$_2$Se nanocrystals [21,35]. According to the relationship of the band gap energy ($E_g$) with the absorption edge, the $E_g$ of the as-prepared Ag$_2$Se nanoparticles was calculated as 1.95 eV, and this value agrees well with the value reported [21,35].

Fig. 5b shows the photoluminescence (PL) spectra of oleic acid capped Ag$_2$Se nanoparticles in n-hexane, with the



**Fig. 4 – FTIR spectra of pure oleic acid (OA) and Ag₂Se nanoparticles.**
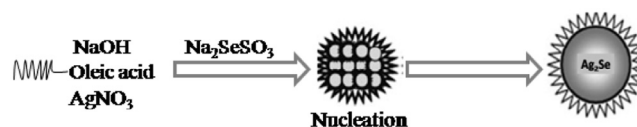


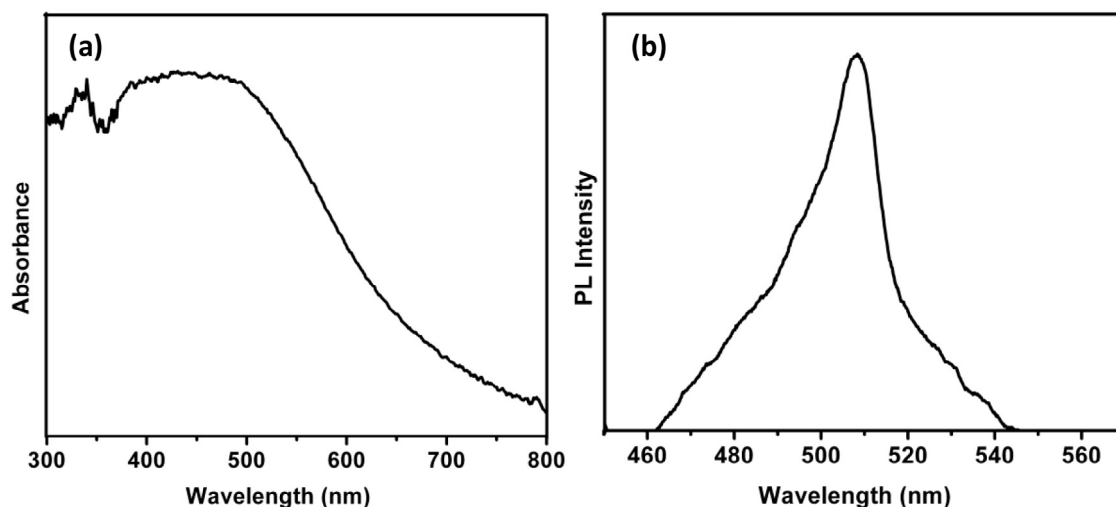**Scheme 1 – The role of oleic acid in the formation of Ag₂Se nanoparticles at low temperature.**

**Fig. 5 – UV–visible absorption (a) and PL spectra (b) of a solution of Ag$_2$Se in n-hexane.**

maximum PL intensity observed at around $\lambda_{max}$ = 510 nm that may result from the direct interband radiative recombination [1].

## 4. Conclusions

In this work, a low-temperature, facile and fast synthesis strategy for nearly monodisperse orthorhombic phase Ag$_2$Se nanoparticles was developed. The optical properties, structure, morphology and other properties of the as-prepared samples were characterized by different instruments such as TEM, FTIR, UV–visible, PL, EDX and XRD. The characterization results of this instrument supported the formation of oleic acid capped orthorhombic phase β-Ag$_2$Se nanoparticles.

In general, to prepare uniform nanoparticles, the developed synthesis strategy has a number of advantages. Firstly, the synthesis of nanoparticles is completed at lower temperature in one-pot makes the system easy to control and manipulate. Secondly, it is a fast method of synthesis to prepare nanoparticles, and this makes the system economical. Thirdly, it is an ideal and general synthesis strategy in making other uniform nanoparticles for mass production through simple precipitation reactions. Last, but not least, this low temperature synthesis protocol is suitable for application in many other materials such as sulfides, fluorides, phosphates and so on, provided that high crystallinity is not required.

## Acknowledgement

REFERENCES

[1] Zhang S-Y, Fang C-X, Wei W, Jin B-K, Tian Y-P, Shen Y-H, et al. Synthesis and electrochemical behavior of crystalline Ag$_2$Se nanotubes. J Phys Chem C 2007;111:4168–74.

[2] Ge J-P, Xu S, Liu L-P, Li Y-D, Positive-Microemulsion A. Method for preparing nearly uniform Ag$_2$Se nanoparticles at low temperature. Chem Eur J 2006;12:3672–7.

[3] Gates B, Mayers B, Wu Y, Sun Y, Cattle B, Yang P, et al. Synthesis and characterizations of crystalline Ag$_2$Se nanowires through a template-engaged reaction at room temperature. Adv Funct Mater 2002;12:679–86.

[4] Okereke NA, Ekpunobi AJ. Structural and electrical characteristics of silver selenide thin films. J Optoelectron Biomed Mater 2011;3:51–5.

[5] Das VD, Karunakaran D. Variations of energy gap, resistivity, and temperature coefficient of resistivity in annealed beta-Ag$_2$Se thin films. Phys Rev B 1989;39:10872–8.

[6] Glanville YJ, Narehood DG, Sokol PE, Amma A, Mallouk T. Preparation and synthesis of Ag$_2$Se nanowires produced by template directed synthesis. J Mater Chem 2002;12:2433–4.

[7] Ng MT, Boothroyd C, Vittal JJ. Shape and size control of Ag$_2$Se nanocrystals from a single precursor [(Ph$_3$P)$_3$Ag$_2$(SeC{O}Ph)$_2$]. Chem Comm 2005;3820–2.

[8] Cui Y, Chen G, Ren J, Shao M, Xie Y, Qian Y. Solvothermal syntheses of beta-Ag2Se crystals with novel morphologies. J Solid State Chem 2003;172:17–21.

[9] Ferhat M, Nagao J. Thermoelectric and transport properties of beta-Ag$_2$Se compounds. J Appl Phys 2000;88:813–16.

[10] Xu R, Husmann A, Rosenbaum TF, Saboungi ML, Enderby JE, Littlewood PB. Large magnetoresistance in non-magnetic silver chalcogenides. Nature 1997;390:57–60.

[11] Kreutzbruck M, Mogwitz B, Gruhl F, Kienle L, Korte C, Janek J. Magnetoresistance in Ag$_{2+\delta}$Se with high silver excess. Appl Phys Lett 2005;86:072 102.

[12] Abrikosov AA. Coherent versus incoherent resonant tunneling in high-T$_c$ cuprates. Phys Rev B 1998;58(13):2788–90.

[13] Moshtaghi S, Zinatloo-Ajabshir S, Salavati-Niasari M. Preparation and characterization of BaSnO$_3$ nanostructures via a new simple surfactant-free route. J Mater Sci: Mater Electron 2016;27:425–35.

[14] Sobhani A, Salavati-Niasari M. Morphological control of MnSe₂/Se nanocomposites by amount of hydrazine through a hydrothermal process. Mater Res Bull 2013;48:3204–10.

[15] Wang W, Geng Y, Qian Y, Ji M, Xie Y. A novel room temperature method to nanocrystalline Ag₂Se. Mater Res Bull 1999;34:877–82.

[16] Harpeness R, Palchik O, Gedanken A, Palchik V, Amiel S, Slifkin MA, et al. Preparation and characterization of Ag₂E (E = Se, Te) using the sonochemically assisted polyol method. Chem Mater 2002;14(5):2094–102.

[17] Ma X-D, Qian X-F, Yin J, Zhu Z-K. Preparation and characterization of polyvinyl alcohol–selenide nanocomposites at room temperature. J Mater Chem 2002;12:663–6.

[18] Ayele DW, Chen H-M, Su W-N, Pan C-J, Chen L-Y, Chou H-L, et al. Controlled synthesis of CdSe quantum dots by a microwave-enhanced process: a green approach for mass production. Chem Eur J 2011;17:5737–44.

[19] Quinlan FT, Kuther J, Tremel W. Reverse micelle synthesis and characterization of ZnSe nanoparticles. Langmuir 2000;16(8):4049–51.

[20] Ingert D, Pileni MP. Limitations in producing nanocrystals using reverse micelles as nanoreactors. Adv Funct Mater 2001;11(2):136–9.

[21] Xiao J, Xie Y, Tang R, Luo W. Template-based synthesis of nanoscale Ag₂E (E = S, Se) dendrites. J Mater Chem 2002;12:1148–51.

[22] Jiang ZY, Huang RB, Xie SY, Xie ZX, Zheng LS. Synthesis of silver selenide bicomponent nanoparticles by a novel technique: laser–solid–liquid ablation. J Solid State Chem 2001;160(2):430–4.

[23] Yan YL, Qian XF, Xu HJ, Yin J, Zhu ZK. A novel solid–liquid route for the preparation of Cu₃Se₂ and Ag₂Se nanocrystals. Inorg Chem Commun 2003;6(1):34–7.

[24] Jiang Y, Xie B, Wu J, Yuan S, Wu Y, Huang H, et al. Synthesis of copper and silver, nanocrystalline chalcogenides in mixed solvents. J Solid State Chem 2002;167(1):28–33.

[25] Batabyal SK, Basu C, Das AR, Sanyal GS. Micropatterns of Ag₂Se nanocrystals. Cryst Growth Des 2004;4(3):509–11.

[26] Gates B, Wu Y, Yin Y, Yang P, Xia Y. Single-crystalline nanowires of Ag₂Se can be synthesized by templating against nanowires of trigonal Se. J Am Chem Soc 2001;123(46):11500–1.

[27] Zhao L-L, Gao Z-M, Liu H, Yang J, Qiaoab S-Z, Du X-W. Modify the morphology of colloidal Ag₂Se nanostructures by laser irradiation. CrystEngComm 2013;15:1685–8.

[28] Cao H, Xiao Y, Lu Y, Yin J, Li B, Wu S, et al. Ag₂Se complex nanostructures with photocatalytic activity and superhydrophobicity. Nano Res. 2010;3:863–73.

[29] Ayele DW, Su W-N, Chou H-L, Pan C-J, Hwang B-J. Composition-controlled optical properties of colloidal CdSe quantum dots. Appl Surf Sci 2014;322:177–84.

[30] Wu N, Fu L, Su M, Aslam M, Wong KC, Dravid VP. Interaction of fatty acid monolayers with cobalt nanoparticles. Nano Lett 2004;4:383–6.

[31] Limaye MV, Singh SB, Date SK, Kothari D, Reddy VR, Gupta A, et al. High coercivity of oleic acid capped CoFe₂O₄ nanoparticles at room temperature. J Phys Chem B 2009;113:9070–6.

[32] Moshtaghi S, Zinatloo-Ajabshir S, Salavati-Niasari M. Nanocrystalline barium stannate: facile morphology-controlled preparation, characterization and investigation of optical and photocatalytic properties. J Mater Sci: Mater Electron 2016;27:834–42.

[33] Zinatloo-Ajabshir S, Salavati-Niasari M, Hamadanian M. Preparation of nanocrystalline praseodymium oxide with different shapes via a simple thermal decomposition route. J Mater Sci: Mater Electron 2016;27:998–1006.

[34] Zinatloo-Ajabshir S, Salavati-Niasari M. Synthesis of pure nanocrystalline ZrO₂ via a simple sonochemical-assisted route. J Ind Eng Chem 2014;20:3313–19.

[35] Pejova B, Najdoski M, Grozdanov I, Dey SK. Chemical bath deposition of nanocrystalline (111) textured Ag₂Se thin films. Mater Lett 2000;43(5–6):269–73.